

1 **Sentinel lead pipe racks quantify orthophosphate's dose-** 2 **response in drinking water**

3 Benjamin F. Trueman^{§,*}, Wendy H. Krkošek[†], and Graham A. Gagnon[§]

4 [§]Centre for Water Resources Studies, Department of Civil & Resource Engineering,
5 Dalhousie University, 1360 Barrington St., Halifax, Nova Scotia, Canada B3H 4R2

6

7 [†]Halifax Water, 450 Cowie Hill Rd., Halifax, Nova Scotia, Canada, B3P 2V3

8

9 *Corresponding author

10 E-mail: benjamin.trueman@dal.ca

11 [Tel:902.494.6070](tel:902.494.6070)

12 [Fax: 902.494.3105](tel:902.494.3105)

13 **Abstract**

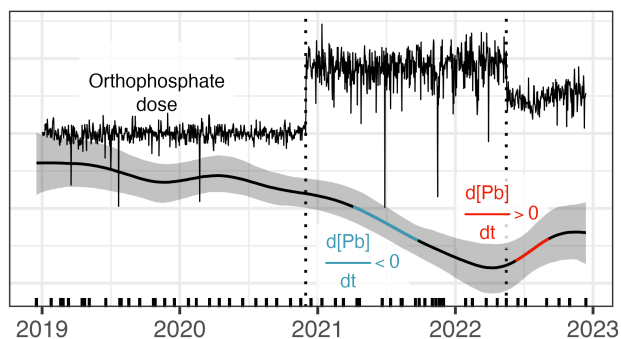
14 Orthophosphate is used to minimize lead contamination of tap water, but its benefits are
15 difficult to quantify since lead concentrations are plumbing-dependent. Homes serviced
16 by lead pipe are ideal for monitoring orthophosphate treatment, but best practices
17 dictate the removal of lead once identified, which complicates sampling plans. Here we
18 explore an alternative: recovered lead pipe racks supplied with distributed drinking
19 water at various locations within a water system. We also propose a strategy for
20 analyzing the data based on the generalized additive model, which approximates time
21 series as a sum of smooth functions. In this study, geometric mean lead release from
22 pipe racks exhibited a pronounced dose-response, falling by 54% after an increase from
23 1 to 2 mg PO₄ L⁻¹, and then climbing by 55% after a decrease to 1.5 mg PO₄ L⁻¹. Data
24 from nine sentinel homes were consistent with those from pipe racks: geometric mean
25 lead at the high orthophosphate dose was 60% of that at the low dose. Our results
26 demonstrate sentinel pipe racks as a viable alternative to at-the-tap sampling for non-
27 regulatory corrosion control monitoring. They also provide a Bayesian framework for
28 quantifying orthophosphate's effect on lead release that can incorporate information
29 from multiple sources.

30 *Keywords:* EPA LCRR; Health Canada; corrosion control; generalized additive model;
31 Bayesian multilevel model

32 **Synopsis**

33 Sentinel pipe racks can be used to quantify the impact of planned and unplanned water
34 quality changes on lead release.

35 **Graphical abstract**



36

37 **Introduction**

38 Updated regulations on lead in drinking water promise to expedite replacement of lead
39 service lines in Canada and the USA. Even afterwards, though, a substantial legacy of
40 lead plumbing—including lead:tin solder and brass—will have to be managed. This will
41 require careful control of drinking water chemistry to limit lead solubility and maintain
42 durable corrosion scale.

43 Orthophosphate is an important tool to that end.^{1–4} It works by forming low-solubility
44 lead-phosphate minerals like pyromorphite ($\text{Pb}_5(\text{PO}_4)_3(\text{Cl},\text{F},\text{OH})$)⁵ and
45 phosphohedyphane ($\text{Ca}_2\text{Pb}_3(\text{PO}_4)_3(\text{Cl},\text{F},\text{OH})$).⁶ Sometimes, it can be effective without
46 forming a lead-phosphate phase,⁷ perhaps by blocking active sites on lead carbonate

47 surfaces^{8,9} or by forming an amorphous diffusion barrier with iron, aluminum,
48 manganese, or calcium.^{10,11}

49 It can be difficult, though, to estimate orthophosphate's effect on lead in drinking water
50 since lead concentrations are determined by site-specific plumbing characteristics.¹²
51 And while modeling can be informative, it generally fails to account for the complex
52 mineralogy of lead corrosion scale or—with notable exceptions¹³—the generation of
53 particles.^{11,14} A decrease in tap water lead sampled at sentinel homes over time is the
54 most reliable metric of orthophosphate's success, and homes supplied by lead service
55 lines represent the population most at-risk.¹⁵ But to protect the inhabitants' health, lead
56 pipe is often replaced once identified. Sentinel homes, then, may have too short a life to
57 be useful in monitoring plumbosolvency changes.

58 Here we describe an alternative: sentinel lead pipe racks supplied with drinking water
59 directly from the distribution system. While they overlap in form and function with pipe
60 loops and bench apparatus, sentinel pipe racks are designed to estimate lead release
61 from representative lead pipes into distributed drinking water with as much precision
62 and accuracy as possible—in as close to real-time as possible. Sentinel pipe racks can
63 be used to understand the effect of an unplanned change in water quality, whereas pipe
64 loop and bench-top studies are usually designed with a specific research question in
65 mind. And while no simple model can fully replicate the complexities of premises
66 plumbing,¹⁶ pipe rack systems are probably a better approximation than benchtop
67 apparatus.¹⁷

68 We present data from three separate racks, located at three sites within the Halifax
69 Regional Municipality, a medium-sized Canadian city. We used a robust hierarchical
70 Bayesian generalized additive model with continuous-time autoregressive errors¹⁸ to
71 estimate the effect on lead release of a dose increase from 1 to 2 mg PO₄ L⁻¹. Then, we
72 used this estimate as a prior probability for the same effect in nine sentinel homes.
73 Finally, we quantified the orthophosphate dose response of a subset of the pipe racks at
74 1, 2, and then 1.5 mg PO₄ L⁻¹. Our results provide a Bayesian framework for analyzing

75 corrosion control treatment data, especially when they are collected as time series and
76 have multiple sources.

77 **Materials and methods**

78 Data were collected in a single water system with two zones supplied by different
79 source waters and treatment plants. Zone 1 is supplied by a conventional treatment
80 plant employing alum coagulation, flocculation, clarification, and filtration. Zone 2 is
81 supplied by a plant employing alum coagulation, flocculation, and direct filtration. Across
82 the two zones, thousands of lead service lines remain, all of which will be replaced by
83 2038 as a part of the utility's comprehensive replacement program.¹⁹

84 **Water quality**

85 Water quality from both sources is well suited to orthophosphate corrosion control
86 treatment,^{20,21} with a pooled median pH and dissolved inorganic carbon concentration in
87 pipe rack effluent of 7.3 and 4.4 mg C L⁻¹ (Table 1). And while water quality in Zones 1
88 and 2 was largely similar, aluminum concentrations were markedly different: aluminum
89 in Zone 2 was seasonal, with peak concentrations occurring at the coldest water
90 temperatures.²² Aluminum concentrations in Zone 1 were much lower and more
91 consistent throughout the year (Table S1).

92 **Table 1.** Summary of water quality in pipe rack effluent; these pooled estimates represent both
93 zones (zone-specific water quality is summarized in Table S1).

Parameter	Unit	Median	Lower quartile	Upper quartile
Dissolved Chloride	mg L ⁻¹	8.4	7.9	9.4
Dissolved Inorganic Carbon	mg C L ⁻¹	4.4	4.1	4.9
Free Chlorine	mg L ⁻¹	0.7	0.2	0.8
Total Organic Carbon	mg C L ⁻¹	1.8	1.7	2.0
pH		7.3	7.2	7.4
Turbidity	NTU	0.1	0.1	0.2

94 **Data collection**

95 **Sentinel pipe racks**

96 Pipe racks were installed in utility-owned infrastructure; two were located in Zone 1 and
97 one in Zone 2. Each was fitted with four replicate recovered lead pipe sections, supplied
98 in parallel with water from the distribution system (an example is shown in Figure S1).
99 Each pipe was excavated and handled according to principles outlined in a recent
100 paper²³ and was approximately 60 cm long with an internal diameter of 1.3 cm. Each
101 was connected to plastic tubing at either end with a brass compression fitting, yielding
102 two galvanic lead-brass connections per pipe. A timed valve supplied flow to the pipe
103 sections for two minutes every six hours, and samples were collected approximately
104 monthly, as the valves opened, at a nominal flow rate of 8 L min⁻¹.

105 **Sentinel homes**

106 Of the nine sentinel homes, seven were supplied by partial lead service lines (private
107 lead, public copper) and the remaining two by copper service lines; all were located in
108 Zone 2. At each sampling round, volunteer residents collected four consecutive 1L
109 samples, starting with the first-draw after a minimum six-hour stagnation period. This 4
110 × 1L profile was followed first by a 10-minute flush of the plumbing and then by
111 collection of a final 1L sample. Sample profiles were collected in May–June 2021, at 1
112 mg PO₄ L⁻¹, and again in May–June 2022, at 2 mg PO₄ L⁻¹. An example instruction
113 sheet provided to residents is included as Figure S2. During the study, all residents
114 were provided with pitcher filters certified by NSF for removal of lead.

115 **Analytical methods**

116 An accredited laboratory measured lead, iron, manganese, zinc, and aluminum,²⁴ as
117 well as dissolved inorganic and total organic carbon,²⁵ chloride,²⁶ sulfate,²⁷
118 orthophosphate,²⁸ and alkalinity²⁹ in pipe rack effluent samples. Turbidity, pH, free
119 chlorine, temperature, conductivity, dissolved oxygen, and oxygen reduction potential

120 were determined onsite using portable Hach instruments. Orthophosphate was also
 121 quantified²⁸ in treated water by Zone 1 and 2 treatment plant staff.

122 **Data analysis**

123 We used R,³⁰ and a collection of contributed packages,^{31–45} to analyze and visualize the
 124 data. Materials (R code and data) necessary to reproduce the main results of the paper
 125 are available online.⁴⁶

126 **Sentinel pipe racks**

127 Lead in pipe rack effluent, y_t , was modeled using a robust hierarchical Bayesian
 128 generalized additive model (GAM) with continuous-time first-order autoregressive
 129 errors.^{18,47–49} The model is specified in equation (1),

$$\text{likelihood:} \\ \log(y_t) \sim T(\mu_t, \sigma, \nu)$$

model for μ_t :

$$\mu_t = \alpha_{pipe_i} + \sum_{j=1}^n f_j(t) + \phi^s r_{t-s} \\ f_j(t) = X_j \beta_j + Z_j b_j$$

$$r_{t-s} = \log(y_{t-s}) - \alpha_{pipe_i} - \sum_{j=1}^n f_j(t-s)$$

130 (1)

priors:

$$\sigma \sim \text{Half-T}(0, 2.5, 3) \\ \nu \sim \text{Gamma}(2, 0.1) \\ \phi \sim N(0.5, 0.25) \\ \alpha_{pipe_i} \sim N(\bar{\alpha}, \sigma_\alpha) \\ \bar{\alpha} \sim T(4.2, 2.5, 3) \\ \sigma_\alpha \sim \text{Half-T}(0, 2.5, 3) \\ \beta_j \sim T(0, 2.5, 3) \\ b_j \sim N(0, \sigma_b) \\ \sigma_b \sim \text{Half-T}(0, 2.5, 3)$$

131 where T denotes the Student t-distribution with time-varying mean μ_t , standard
132 deviation σ , and degrees-of-freedom parameter ν . The mean is modeled as the sum of
133 smooth functions of time $f_j(t)$. The full model (Zones 1 and 2) included a pipe-specific
134 intercept α_{pipe_i} and centered smooth terms, whereas the Zone 1 model included non-
135 centered series-specific smooths and a global intercept ($\bar{\alpha}$ in place of α_{pipe_i} in equation
136 (1)). The matrices Z_j and X_j represent the penalized and unpenalized basis functions
137 comprising each of the $f_j(t)$, and b_j and β_j represent the penalized and unpenalized
138 GAM coefficients. The parameter ϕ is the first-order autoregressive coefficient, and s
139 represents the spacing in time between consecutive observations. Γ and N
140 denote the gamma and normal distributions.

141 On the log scale, the time-varying mean in the full model was estimated as the sum of a
142 global multi-year trend, a set of local multi-year trends modifying the global trend to
143 better fit the data from each location, and a second set of local multi-year trends
144 capturing deviations of the individual time series from the global and location-level
145 trends (Figure S3a). Since orthophosphate was increased on different dates in Zones 1
146 and 2, we expressed time as days before and after the respective increases. The time-
147 varying mean in the Zone 1 model was estimated as the sum of a global multi-year
148 trend, a seasonal trend, and a set of local multi-year trends capturing deviations of the
149 individual time series from the global and seasonal trends (Figure S4). In both models,
150 the multi-year trends were estimated using thin-plate regression splines, and the Zone 1
151 model's seasonal trend was estimated using a cyclic cubic regression spline.⁴⁵

152 The instantaneous rate of change in mean log lead concentration was estimated using
153 finite differences, as described in a recent paper.¹⁸ Briefly, we generated posterior
154 predictions of the global or location-level multi-year trend along a regular time sequence
155 spanning the range of the data. Then, we repeated this process after adding a small δ
156 to each value in the sequence. The difference between posterior predictions evaluated
157 at t and $t + \delta$, divided by δ , approximates the first derivative of the smooth term.

158 **Sentinel homes**

159 Lead concentrations in point-of-use samples, y_i , were described using a multilevel
 160 model.⁵⁰ That is, the change in lead release accompanying the orthophosphate dose
 161 increase was estimated after accounting for the effects of sample location and profile
 162 litre. The model is specified in equation (2),

$$\begin{aligned}
 & \text{likelihood:} \\
 & \log(y_i)|_{\text{censored} = 0} \sim T(\mu_i, \sigma, \nu) \\
 & \log(y_i)|_{\text{censored} = 1} \sim T\text{-CDF}(\mu_i, \sigma, \nu) \\
 & \text{model for } \mu_i: \\
 & \mu_i = \alpha_{\text{site}_j} + \gamma_{\text{sample}_k} + \beta R \\
 & \text{priors:} \\
 163 \quad (2) \quad & \sigma \sim \text{Half-N}(0,1) \\
 & \nu \sim \text{Gamma}(2,0.1) \\
 & \beta \sim N(-0.8,0.3) \\
 & \alpha_{\text{site}_j} \sim N(\bar{\alpha}, \sigma_\alpha), \text{ for } j \text{ in } 1..9 \\
 & \bar{\alpha} \sim N(0,1) \\
 & \sigma_\alpha \sim \text{Half-Cauchy}(0,1) \\
 & \gamma_{\text{sample}_k} \sim N(0, \sigma_\gamma), \text{ for } k \text{ in } 1..45 \\
 & \sigma_\gamma \sim \text{Half-Cauchy}(0,1)
 \end{aligned}$$

164 where T again denotes the Student t-distribution with mean μ , standard deviation σ , and
 165 degrees-of-freedom ν ; *censored* is a binary variable indicating whether the sample
 166 concentration was observed or left-censored (i.e., a nondetect). The parameters α_{site_j}
 167 and γ_{sample_k} are random intercepts describing each unique site/profile litre combination,
 168 R is a binary variable indicating the sampling round (i.e., before/after the dose increase),
 169 and β is the difference between rounds. *Half-Cauchy*, and *T-CDF* represent the half-
 170 Cauchy distribution and the Student t cumulative distribution function (i.e., $P(X \leq x)$).
 171 *T-CDF* quantifies the probability that y_i is less than the censoring limit on the log scale.
 172 Nondetects, then, inform the model without the need to replace them with imputed
 173 values.

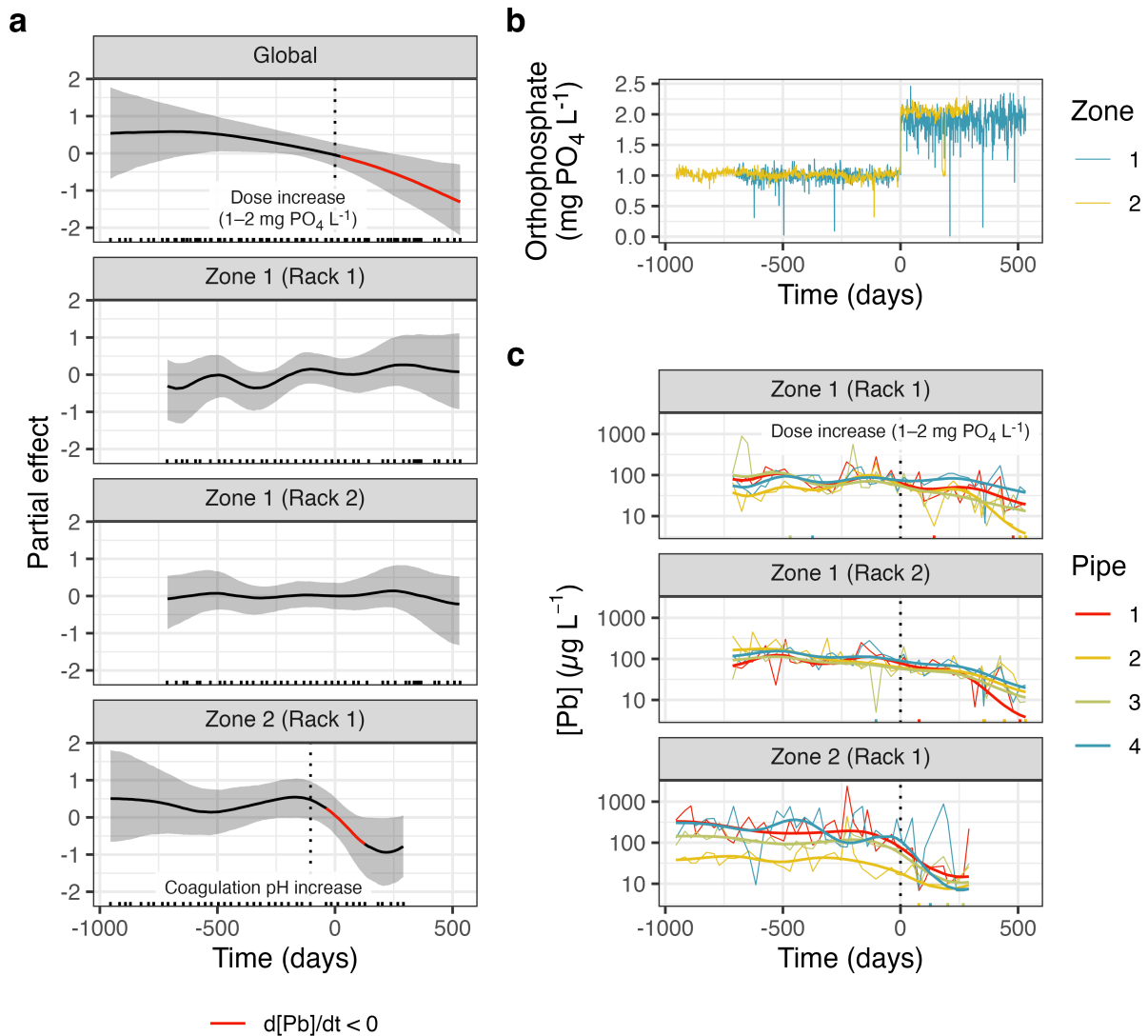
174 The priors on $\bar{\alpha}$, σ_{α} , and σ_{γ} are weakly informative, meaning that they discourage
175 unrealistic parameter estimates.⁵¹ The prior on β —the difference between lead
176 concentration at the two orthophosphate doses—was determined using posterior
177 predictions from the generalized additive model of pipe loop data, as described in the
178 Results and discussion.

179 **Results and discussion**

180 **Quantifying the effect of an orthophosphate dose increase**

181 **Sentinel pipe racks**

182 Lead release from pipe racks was relatively constant at 1 mg PO₄ L⁻¹ (Figure 1c). At this
183 dose, a 95% credible interval on the slope of the global multi-year trend—capturing
184 variation common to all pipe sections—included 0 μg Pb L⁻¹ d⁻¹ at all times (d[Pb]/dt ~ 0,
185 Figure 1a). Pipe racks, then, appear to have been successfully stabilized at the initial
186 orthophosphate concentration.



187

188 **Figure 1. (a)** The global multi-year smooth term representing the change in lead concentration
 189 across all pipe sections, and the local modifiers representing deviations from the global trend to
 190 better fit data from each pipe rack. Red highlighting indicates the portion of the trend where a
 191 95% credible interval on its slope does not include zero, and the shaded grey region represents
 192 a 95% credible interval on the time-varying mean. Sample collection dates are indicated by
 193 vertical ticks on the x-axis. **(b)** Orthophosphate in treated water, by zone. **(c)** Time series of total
 194 lead in effluent from lead pipes at three locations. Fitted values from the hierarchical GAM are
 195 superimposed on the time series in bold. Ticks at the top and bottom of the panels represent
 196 values outside the plotting limits.

197 An increase to 2 mg PO₄ L⁻¹ was followed by a decreasing trend in lead concentration
 198 (Figure 1a, c). That is, a 95% credible interval on the slope of the global multi-year trend
 199 excluded 0 μg Pb L⁻¹ d⁻¹ for a period beginning shortly after the dose increase and

200 running until the end of the study period ($d[\text{Pb}]/dt < 0$, Figure 1a). The higher dose, then,
201 appeared to provide additional protection against lead release. Across both zones and
202 all three pipe racks, doubling the orthophosphate dose decreased the geometric mean
203 lead concentration within a year by an estimated 54% (95% credible interval: 14–77%).

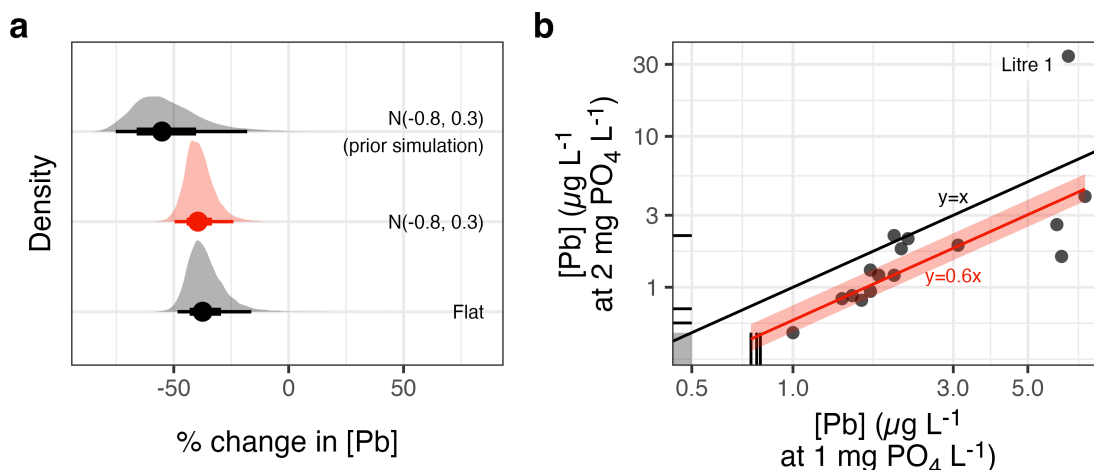
204 An additional decrease in lead release was particular to Zone 2 and not accounted for
205 by the global trend (Figure 1a). A possible explanation was a modified treatment
206 process: coagulation pH at the Zone 2 treatment plant was increased from less than 6
207 to approximately 6.3 in April 2021 (Figure S3b), to target the pH of minimum aluminum
208 hydroxide solubility.⁵² This lowered aluminum in treated water (Figure S5), and a
209 decrease in the aluminum concentration predicts a decrease in lead solubility—
210 assuming that some fraction of dissolved aluminum precipitates with orthophosphate,
211 leaving less available to react with lead.²² Less aluminum in solution may also mean
212 less post-precipitation of aluminum as particles and less adsorption of lead to those
213 particles. And since suspended colloids containing aluminum and lead have been
214 identified in Zone 2,²² the increase in coagulation pH may have decreased the capacity
215 of distributed water to transport lead. Moreover, an improved coagulation process would
216 be expected to remove more of the natural organic matter fractions that increase lead
217 solubility by complexation.⁵³ These fractions, though, were not measured in treated
218 water.

219 The decrease in the location-specific trend representing Zone 2 followed closely the
220 increase in coagulation pH, and neither of the Zone 1 trends decreased comparably
221 (Figure 1b). Furthermore, a 95% credible interval on the slope of the Zone 2 trend
222 excluded $0 \mu\text{g Pb L}^{-1} \text{d}^{-1}$ for several months, beginning shortly after the pH increase
223 ($d[\text{Pb}]/dt < 0$, Figure 1b). Changes to the coagulation process, then, appear to have
224 lowered lead release: between the coagulation pH increase and the orthophosphate
225 dose increase, geometric mean lead decreased by an estimated 34% (95% credible
226 interval: 0–57%). And since only a short period separated the pH increase and the
227 change in orthophosphate dose, controlling for orthophosphate's effect yielded a more
228 reliable estimate of the coagulation pH effect. That is, the hierarchical nature of the

229 model allows us to control for an effect common to all groups to better understand an
230 effect that occurred in only one group.

231 Sentinel homes

232 We used the estimated year-over-year decrease in geometric mean lead release from
233 pipe racks (54%) as a prior probability for orthophosphate's effect on lead
234 concentrations in the sentinel homes' tap water (Figure 2a). The prior probability reflects
235 our state of knowledge before learning from the point-of-use data; on the natural log
236 scale, an approximation of the prior difference estimate is $N(\mu = -0.8, \sigma = 0.3)$, where
237 N is a Gaussian with mean μ and standard deviation σ .



238

239 **Figure 2. (a)** Density plots show the estimated percent change in lead at the point of use,
240 comparing sample profiles collected at 1 mg PO₄ L⁻¹ and again, approximately 1 year later, at 2
241 mg PO₄ L⁻¹. Model predictions generated using a flat prior (i.e., no prior knowledge of the effect
242 of orthophosphate) are compared against those generated using a prior informed by the GAM.
243 (N denotes the normal distribution.) **(b)** Lead at the point of use, paired by site and profile litre.
244 Left-censored values (i.e., nondetects) are represented by the horizontal/vertical ticks and the
245 grey-shaded region at the bottom left of the plot. The red diagonal line represents the estimated
246 difference between lead concentrations at the two doses, and the red-shaded region represents
247 a 95% credible interval on that estimate (generated using an informative $N(-0.8, 0.3)$ prior).

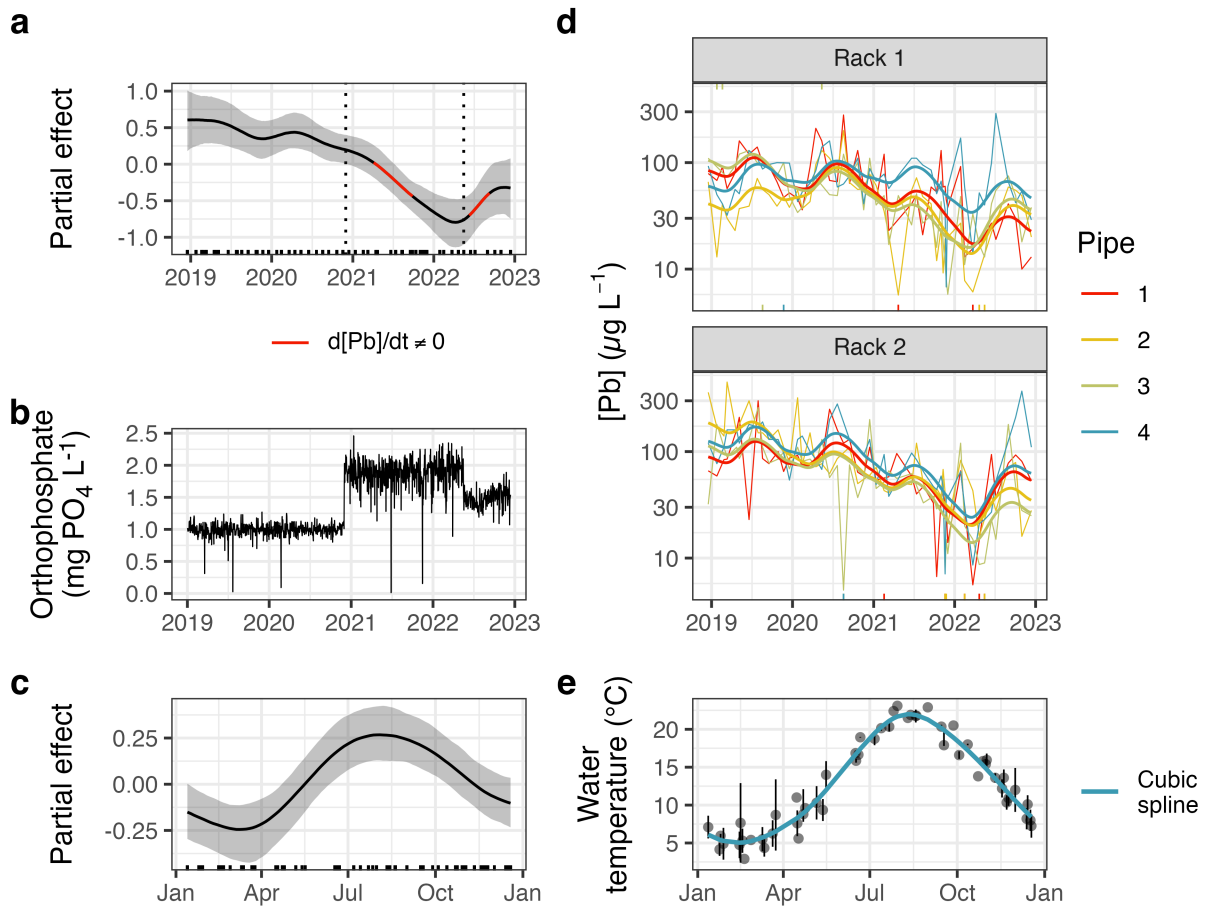
248 Geometric mean lead release at the high orthophosphate dose (2 mg PO₄ L⁻¹) was 60%
249 of that at the low dose (1 mg PO₄ L⁻¹), with a 95% credible interval of 50–76% (Figure
250 2b). The choice of prior had little influence on the difference estimate: the corresponding

251 estimate obtained by using an uninformative prior—assigning equal probability to all
252 orthophosphate treatment effect sizes, whether physically plausible or not—was 63%,
253 with a 95% credible interval of 52–84%.

254 These estimates are somewhat smaller than the one based on pipe rack data.
255 Differences in the models are a factor, but differences in materials also matter. That is,
256 pipe racks measure the response of lead pipe to orthophosphate treatment, which tends
257 to be quite large at slightly basic pH and low dissolved inorganic carbon.²⁰ Data from
258 sentinel homes, though, also capture the effect of orthophosphate on lead release from
259 other sources, which is much more ambiguous. Corrosion of lead solder, for instance,
260 may be accelerated by orthophosphate.⁵⁴ To capture these effects, pipe racks could
261 easily be modified to include copper and lead solder.

262 **Quantifying the effect of an orthophosphate dose decrease**

263 A little more than a year after the orthophosphate dose was increased in Zone 1, it was
264 decreased from 2 to 1.5 mg PO₄ L⁻¹ (Figure 3b). We used the sentinel pipe racks to
265 determine the orthophosphate dose response in this zone. That is, we estimated the
266 effect of an increase from 1 to 2 mg PO₄ L⁻¹ and the effect of a subsequent decrease to
267 1.5 mg PO₄ L⁻¹. But since the final decrease occurred in the spring—as water
268 temperatures were increasing rapidly (Figure 3e)—we estimated the seasonal variation
269 in lead release and added it as a separate term in the model to control for temperature
270 effects. Seasonality was more complex in Zone 2, perhaps due to the inverse
271 seasonality in aluminum (especially before the change in coagulation pH²²). And since
272 the dose increases occurred in late November and July in Zones 1 and 2 respectively,
273 controlling explicitly for seasonality in the full model—encompassing both zones—was
274 less important.



275

276 **Figure 3.** (a) The global multi-year trend in lead release; red highlighting indicates the portion of
 277 the trend where the 95% credible interval on its slope does not include zero. (b)
 278 Orthophosphate in Zone 1 treated water. (c) The seasonal smooth term in the GAM. In (a) and
 279 (c), shaded grey regions span 95% credible intervals on the trends, and ticks on the x-axes
 280 represent sample collection dates. (d) Time series of total lead in effluent from lead pipes at the
 281 two locations in Zone 1. Fitted values from the hierarchical GAM are superimposed on the time
 282 series in bold. Ticks at the top and bottom of the panels represent values outside the plotting
 283 limits. (e) Water temperature in pipe rack effluent; points represent medians and error bars span
 284 the range of measurements, by date. A cyclic cubic spline⁴⁸ is superimposed in blue.

285 As in the full model, mean (log) lead concentrations were relatively constant at 1 mg
 286 PO₄ L⁻¹: at this dose, a 95% credible interval on the slope of the global multi-year trend
 287 always included 0 μg Pb L⁻¹ d⁻¹ (Figure 3a). An increase to 2 mg PO₄ L⁻¹ was followed
 288 here as well by a decreasing trend in lead concentrations.

289 Even after accounting for the seasonal variation in lead release, though, a decrease in
 290 the orthophosphate dose to 1.5 mg PO₄ L⁻¹ was followed by an increase in lead release

291 (Figure 3a) and a 95% credible interval on the slope of the global trend that did not
292 include zero. The intermediate dose, then, appears to have yielded lead concentrations
293 between those resulting from the 1 and 2 mg PO₄ L⁻¹ doses. Six months after the
294 orthophosphate dose reduction, the increase in geometric mean lead release was
295 estimated at 55%, with a 95% credible interval of 5–143%.

296 This result has implications for passivation-maintenance orthophosphate dosing
297 strategies—that is, initiating treatment at a high orthophosphate dose to promote lead
298 phosphate scale formation and then decreasing the dose once scale evolution has
299 slowed.⁵⁵ Although lead solubility is predicted to increase with a decrease in
300 orthophosphate, the effect on particulate lead is unclear: an established lead-phosphate
301 scale, for instance, may be no less durable after a decrease in the orthophosphate
302 dose. But while passivation/maintenance dosing has the potential to conserve
303 phosphorus, it should be evaluated carefully to avoid unwanted increases in lead
304 release at the maintenance dose or excess particulate lead at an unnecessarily high
305 passivation dose.^{18,56} Here, the dose response of lead release to orthophosphate was
306 qualitatively similar to that predicted by solubility: lead release decreased when
307 orthophosphate was increased and increased when orthophosphate was decreased.

308 **Conclusion**

309 Point-of-use sampling is necessary to accurately quantify lead release into drinking
310 water. But lead service line replacement, incomplete participation by residents in
311 sampling programs, and changes to premises plumbing make it difficult to monitor the
312 effectiveness of corrosion control over time this way. And while no simple apparatus can
313 reliably quantify human exposure to lead, sentinel pipe racks offer an alternative to
314 point-of-use sampling for non-regulatory monitoring. Especially when installed at
315 multiple locations across a water distribution network, sentinel pipe racks can be used
316 to understand how both anticipated and unexpected changes in water quality impact
317 lead concentrations. We used them here to estimate the effect on lead release of

318 changes in orthophosphate dose and coagulation process. By partitioning the variation
319 in lead concentrations hierarchically—estimating global and location-level trends—we
320 were better able to control for seasonality or other potential confounders before
321 quantifying the effects of interest.

322 **Acknowledgements**

323 This work was supported by Mitacs, through the Mitacs Accelerate Program (Reference
324 # IT23352), and NSERC, through an Industrial Research Chair program (Grant #
325 IRCPJ: 349838-16). We acknowledge Halifax Water’s water quality department for
326 managing the pipe rack and residential sampling programs.

327 **Supporting information**

328 Graphical and tabular summaries of water quality, figures summarizing smooth terms
329 not appearing in the body of the paper, instructions provided to volunteer residents, and
330 a photo of a prototype pipe rack.

331 **References**

- 332 (1) Schock, M. R. Understanding Corrosion Control Strategies for Lead. *Journal -*
333 *American Water Works Association* **1989**, *81* (7), 88–100.
334 <https://doi.org/10.1002/j.1551-8833.1989.tb03244.x>.
- 335 (2) Dodrill, D. M.; Edwards, M. Corrosion Control on the Basis of Utility Experience.
336 *Journal - American Water Works Association* **1995**, *87* (7), 74–85.
337 <https://doi.org/10.1002/j.1551-8833.1995.tb06395.x>.
- 338 (3) Bae, Y.; Pasteris, J. D.; Giammar, D. E. Impact of Orthophosphate on Lead
339 Release from Pipe Scale in High pH, Low Alkalinity Water. *Water Research*
340 **2020**, *177*, 115764. <https://doi.org/10.1016/j.watres.2020.115764>.
- 341 (4) Doré, E.; Deshommès, E.; Laroche, L.; Nour, S.; Prévost, M. Study of the Long-
342 Term Impacts of Treatments on Lead Release from Full and Partially Replaced
343 Harvested Lead Service Lines. *Water Research* **2019**, *149*, 566–577.
344 <https://doi.org/10.1016/j.watres.2018.11.037>.

- 345 (5) Lytle, D. A.; Schock, M. R.; Formal, C.; Bennett-Stamper, C.; Harmon, S.;
346 Nadagouda, M. N.; Williams, D.; DeSantis, M. K.; Tully, J.; Pham, M. Lead
347 Particle Size Fractionation and Identification in Newark, New Jersey's Drinking
348 Water. *Environmental Science & Technology* **2020**, *54* (21), 13672–13679.
349 <https://doi.org/10.1021/acs.est.0c03797>.
- 350 (6) Bae, Y.; Pasteris, J. D.; Giammar, D. E. The Ability of Phosphate To Prevent
351 Lead Release from Pipe Scale When Switching from Free Chlorine to
352 Monochloramine. *Environmental Science & Technology* **2020**, *54* (2), 879–888.
353 <https://doi.org/10.1021/acs.est.9b06019>.
- 354 (7) Aghasadeghi, K.; Peldszus, S.; Trueman, B. F.; Mishra, A.; Cooke, M. G.;
355 Slawson, R. M.; Giammar, D. E.; Gagnon, G. A.; Huck, P. M. Pilot-Scale
356 Comparison of Sodium Silicates, Orthophosphate and pH Adjustment to Reduce
357 Lead Release from Lead Service Lines. *Water Research* **2021**, *195*, 116955.
358 <https://doi.org/10.1016/j.watres.2021.116955>.
- 359 (8) Noel, J. D.; Wang, Y.; Giammar, D. E. Effect of Water Chemistry on the
360 Dissolution Rate of the Lead Corrosion Product Hydrocerussite. *Water Research*
361 **2014**, *54*, 237–246. <https://doi.org/10.1016/j.watres.2014.02.004>.
- 362 (9) Li, B.; Trueman, B. F.; Locsin, J. M.; Gao, Y.; Rahman, M. S.; Park, Y.; Gagnon,
363 G. A. Impact of Sodium Silicate on Lead Release from Lead(II) Carbonate.
364 *Environmental Science: Water Research & Technology* **2021**, *7* (3), 599–609.
365 <https://doi.org/10.1039/D0EW00886A>.
- 366 (10) Wasserstrom, L. W.; Miller, S. A.; Triantafyllidou, S.; Desantis, M. K.; Schock, M.
367 R. Scale Formation Under Blended Phosphate Treatment for a Utility With Lead
368 Pipes. *Journal - American Water Works Association* **2017**, *109*, E464–E478.
369 <https://doi.org/10.5942/jawwa.2017.109.0121>.
- 370 (11) Tully, J.; DeSantis, M. K.; Schock, M. R. Water Quality–Pipe Deposit
371 Relationships in Midwestern Lead Pipes. *AWWA Water Science* **2019**, *1* (2),
372 e1127. <https://doi.org/10.1002/aws2.1127>.
- 373 (12) Redmon, J. H.; Kondash, A. J.; Norman, E.; Johnson, J.; Levine, K.; McWilliams,
374 A.; Napier, M.; Weber, F.; Stella, L.; Wood, E.; Jackson, C. L. P.; Mulhern, R.
375 Lead Levels in Tap Water at Licensed North Carolina Child Care Facilities,
376 2020–2021. *American Journal of Public Health* **2022**, *112* (S7), S695–S705.
377 <https://doi.org/10.2105/AJPH.2022.307003>.
- 378 (13) Abokifa, A. A.; Biswas, P. Modeling Soluble and Particulate Lead Release into
379 Drinking Water from Full and Partially Replaced Lead Service Lines.
380 *Environmental Science & Technology* **2017**, *51* (6), 3318–3326.
381 <https://doi.org/10.1021/acs.est.6b04994>.
- 382 (14) Trueman, B. F.; Anaviapik-Soucie, T.; L'Hérault, V.; Gagnon, G. A.
383 Characterizing Colloidal Metals in Drinking Water by Field Flow Fractionation.

- 384 *Environmental Science: Water Research & Technology* **2019**, 5 (12), 2202–2209.
385 <https://doi.org/10.1039/C9EW00560A>.
- 386 (15) Health Canada. *Guidance on sampling and mitigation measures for controlling*
387 *corrosion - guidance document for public consultation*.
388 [https://www.canada.ca/en/health-canada/programs/consultation-draft-guidance-](https://www.canada.ca/en/health-canada/programs/consultation-draft-guidance-sampling-mitigation-measures-controlling-corrosion.html)
389 [sampling-mitigation-measures-controlling-corrosion.html](https://www.canada.ca/en/health-canada/programs/consultation-draft-guidance-sampling-mitigation-measures-controlling-corrosion.html) (accessed 2023-01-16).
- 390 (16) Devine, C.; Triantafyllidou, S. A Literature Review of Bench Top and Pilot Lead
391 Corrosion Assessment Studies. *AWWA Water Science* **2023**, 5 (2), e1324.
392 <https://doi.org/10.1002/aws2.1324>.
- 393 (17) Masters, S. V.; Poncelet-Johnson, N.; Walsh, R.; Seidel, C. J.; Corwin, C. J.
394 Comparison of Coupon and Pipe Rack Studies for Selecting Corrosion Control
395 Treatment. *AWWA Water Science* **2022**, 4 (4).
396 <https://doi.org/10.1002/aws2.1293>.
- 397 (18) Trueman, B. F.; James, W.; Shu, T.; Doré, E.; Gagnon, G. A. Comparing
398 Corrosion Control Treatments for Drinking Water Using a Robust Bayesian
399 Generalized Additive Model. *ACS ES&T Engineering* **2022**, 15–25.
400 <https://doi.org/10.1021/acsestengg.2c00194>.
- 401 (19) Krkošek, W.; Healey, M.; Sampson, C.; McKnight, A. Halifax Water’s Lead
402 Service Line Replacement Program Gets the Lead Out. *Journal AWWA* **2022**,
403 *114* (2), 10–19. <https://doi.org/10.1002/awwa.1862>.
- 404 (20) Schock, M. R.; Wagner, I.; Oliphant, R. J. Corrosion and solubility of lead in
405 drinking water. In *Internal corrosion of water distribution systems*; American
406 Water Works Association Research Foundation: Denver, CO, 1996; pp 131–230.
- 407 (21) Trueman, B. F.; Krkošek, W. H.; Gagnon, G. A. Effects of Ortho- and
408 Polyphosphates on Lead Speciation in Drinking Water. *Environmental Science:*
409 *Water Research & Technology* **2018**, 4 (4), 505–512.
410 <https://doi.org/10.1039/C7EW00521K>.
- 411 (22) Trueman, B. F.; Bleasdale-Pollowy, A.; Locsin, J. A.; Bennett, J. L.; Krkošek, W.
412 H.; Gagnon, G. A. Seasonal Lead Release into Drinking Water and the Effect of
413 Aluminum. *ACS ES&T Water* **2022**, 710–720.
414 <https://doi.org/10.1021/acsestwater.1c00320>.
- 415 (23) Harmon, S. M.; Tully, J.; DeSantis, M. K.; Schock, M. R.; Triantafyllidou, S.; Lytle,
416 D. A. A Holistic Approach to Lead Pipe Scale Analysis: Importance,
417 Methodology, and Limitations. *AWWA Water Science* **2022**, 4 (2).
418 <https://doi.org/10.1002/aws2.1278>.
- 419 (24) USEPA. *Method 6020B (SW-846): Inductively Coupled Plasma-Mass*
420 *Spectrometry, Revision 2*; 2014.

- 421 (25) 5310 Total Organic Carbon. In *Standard methods for the examination of water*
422 *and wastewater*. <https://doi.org/10.2105/SMWW.2882.104>.
- 423 (26) 4500-Cl Chloride. In *Standard methods for the examination of water and*
424 *wastewater*. <https://doi.org/10.2105/SMWW.2882.079>.
- 425 (27) ASTM International. *Standard test method for sulfate ion in water*.
426 <https://www.astm.org/d0516-16.html>.
- 427 (28) 4500-P Phosphorus. In *Standard methods for the examination of water and*
428 *wastewater*. <https://doi.org/10.2105/SMWW.2882.093>.
- 429 (29) USEPA. *Method 310.2: Alkalinity (Colorimetric, Automated, Methyl Orange) by*
430 *Autoanalyzer*, 1974.
- 431 (30) R Core Team. *R: A language and environment for statistical computing*.
432 <https://www.R-project.org/>.
- 433 (31) Allaire, J.; Xie, Y.; McPherson, J.; Luraschi, J.; Ushey, K.; Atkins, A.; Wickham,
434 H.; Cheng, J.; Chang, W.; Iannone, R. *rmarkdown: Dynamic documents for R*.
435 <https://github.com/rstudio/rmarkdown>.
- 436 (32) Wickham, H.; Averick, M.; Bryan, J.; Chang, W.; McGowan, L. D.; François, R.;
437 Golemund, G.; Hayes, A.; Henry, L.; Hester, J.; Kuhn, M.; Pedersen, T. L.;
438 Miller, E.; Bache, S. M.; Müller, K.; Ooms, J.; Robinson, D.; Seidel, D. P.; Spinu,
439 V.; Takahashi, K.; Vaughan, D.; Wilke, C.; Woo, K.; Yutani, H. Welcome to the
440 tidyverse. *Journal of Open Source Software* **2019**, 4 (43), 1686.
441 <https://doi.org/10.21105/joss.01686>.
- 442 (33) Wickham, H.; Bryan, J. *readxl: Read excel files*. [https://CRAN.R-](https://CRAN.R-project.org/package=readxl)
443 [project.org/package=readxl](https://CRAN.R-project.org/package=readxl).
- 444 (34) Firke, S. *janitor: Simple tools for examining and cleaning dirty data*.
445 <https://CRAN.R-project.org/package=janitor>.
- 446 (35) Fischetti, T. *assertr: Assertive programming for r analysis pipelines*.
447 <https://CRAN.R-project.org/package=assertr>.
- 448 (36) Bürkner, P.-C. brms: An R Package for Bayesian Multilevel Models Using Stan.
449 *Journal of Statistical Software* **2017**, 80 (1), 1–28.
450 <https://doi.org/10.18637/jss.v080.i01>.
- 451 (37) Kay, M. *ggdist: Visualizations of distributions and uncertainty*.
452 <https://doi.org/10.5281/zenodo.3879620>.
- 453 (38) Hester, J.; Bryan, J. *glue: Interpreted string literals*. [https://CRAN.R-](https://CRAN.R-project.org/package=glue)
454 [project.org/package=glue](https://CRAN.R-project.org/package=glue).
- 455 (39) Bürkner, P.-C.; Gabry, J.; Kay, M.; Vehtari, A. *posterior: Tools for working with*
456 *posterior distributions*. <https://mc-stan.org/posterior/>.

- 457 (40) Wickham, H. *testthat: Get Started with Testing*. *The R Journal* **2011**, 3, 5–10.
- 458 (41) Gabry, J.; Mahr, T. *bayesplot: Plotting for bayesian models*. [https://mc-](https://mc-stan.org/bayesplot/)
459 [stan.org/bayesplot/](https://mc-stan.org/bayesplot/).
- 460 (42) Pedersen, T. L. *patchwork: The composer of plots*. [https://CRAN.R-](https://CRAN.R-project.org/package=patchwork)
461 [project.org/package=patchwork](https://CRAN.R-project.org/package=patchwork).
- 462 (43) Wilke, C. O.; Wiernik, B. M. *ggtext: Improved text rendering support for 'ggplot2'*.
463 <https://CRAN.R-project.org/package=ggtext>.
- 464 (44) Wickham, H.; Hester, J.; Chang, W.; Bryan, J. *devtools: Tools to make*
465 *developing r packages easier*. <https://CRAN.R-project.org/package=devtools>.
- 466 (45) Wood, S. N. *Generalized Additive Models: An Introduction with R*, 2nd ed.;
467 Chapman; Hall/CRC, 2017.
- 468 (46) Trueman, B. *Source code for "Sentinel pipe racks quantify orthophosphate's*
469 *effect on lead release into drinking water"*. [https://github.com/bentrueman/cct-](https://github.com/bentrueman/cct-monitoring)
470 [monitoring](https://github.com/bentrueman/cct-monitoring).
- 471 (47) Trueman, B. *bgamcar1: Fit bayesian GAMs with CAR(1) errors to censored data*.
472 <https://github.com/bentrueman/bgamcar1>.
- 473 (48) Pedersen, E. J.; Miller, D. L.; Simpson, G. L.; Ross, N. Hierarchical Generalized
474 Additive Models in Ecology: An Introduction with mgcv. *PeerJ* **2019**, 7, e6876.
475 <https://doi.org/10.7717/peerj.6876>.
- 476 (49) Simpson, G. L. Modelling Palaeoecological Time Series Using Generalised
477 Additive Models. *Frontiers in Ecology and Evolution* **2018**, 6, 149.
478 <https://doi.org/10.3389/fevo.2018.00149>.
- 479 (50) McElreath, R. *Statistical Rethinking: A Bayesian Course with Examples in R and*
480 *Stan*; Chapman & Hall/CRC texts in statistical science series; CRC Press/Taylor
481 & Francis Group: Boca Raton, 2016.
- 482 (51) Gelman, A. Bayes, Jeffreys, Prior Distributions and the Philosophy of Statistics.
483 *Statistical Science* **2009**, 24 (2). <https://doi.org/10.1214/09-STS284D>.
- 484 (52) Edzwald, J. K. Aluminum in Drinking Water: Occurrence, Effects, and Control.
485 *Journal AWWA* **2020**, 112 (5), 34–41. <https://doi.org/10.1002/awwa.1499>.
- 486 (53) Korshin, G. V.; Ferguson, J. F.; Lancaster, A. N.; Wu, H. *Corrosion and Metal*
487 *Release for Lead-Containing Materials: Influence of NOM*; AWWA Research
488 Foundation; American Water Works Association: Denver, 1999.
- 489 (54) Nguyen, C. K.; Clark, B. N.; Stone, K. R.; Edwards, M. A. Acceleration of
490 Galvanic Lead Solder Corrosion Due to Phosphate. *Corrosion Science* **2011**, 53
491 (4), 1515–1521. <https://doi.org/10.1016/j.corsci.2011.01.016>.

- 492 (55) Schock, M. R.; Clement, J. Lead and Copper Control with Non-Zinc
493 Orthophosphate. *Journal - New England Water Works Association* **1998**, *112*,
494 20–20.
- 495 (56) Zhao, J.; Giammar, D. E.; Pasteris, J. D.; Dai, C.; Bae, Y.; Hu, Y. Formation and
496 Aggregation of Lead Phosphate Particles: Implications for Lead Immobilization in
497 Water Supply Systems. *Environmental Science & Technology* **2018**, *52* (21),
498 12612–12623. <https://doi.org/10.1021/acs.est.8b02788>.

Supplementary information for: Sentinel lead pipe racks quantify orthophosphate's dose-response in drinking water

Benjamin F. Trueman^{§,*}, Wendy H. Krkošek[†], and Graham A. Gagnon[§]

[§]Centre for Water Resources Studies, Department of Civil & Resource Engineering, Dalhousie University, 1360 Barrington St., Halifax, Nova Scotia, Canada B3H 4R2

[†]Halifax Water, 450 Cowie Hill Rd., Halifax, Nova Scotia, Canada, B3P 2V3

*Corresponding author

E-mail: benjamin.trueman@dal.ca

Tel: 902.494.6070

Fax: 902.494.3105

This document has 5 pages, 5 figures, and 1 table.

Table S1. Summary of water quality in pipe rack effluent, by zone.

Parameter	Unit	Zone	Median	Lower quartile	Upper quartile
Conductivity	mS	1	142.0	133.0	153.0
		2	87.0	82.0	93.0
Dissolved Chloride	mg L ⁻¹	1	8.4	7.8	9.2
		2	8.6	7.9	9.6
Dissolved Inorganic Carbon	mg C L ⁻¹	1	4.6	4.3	5.0
		2	3.7	3.3	4.3
Dissolved Sulfate	mg SO ₄ L ⁻¹	1	32.0	29.0	36.0
		2	9.6	8.7	11.0
Dissolved Oxygen	mg L ⁻¹	1	10.0	9.1	11.8
		2	10.2	9.6	12.0
Free Chlorine		1	0.5	0.1	0.7
		2	0.7	0.6	0.8
Total Organic Carbon	mg C L ⁻¹	1	1.8	1.7	2.0
		2	1.8	1.8	2.1
ORP	mV	1	516.0	435.5	624.0
		2	422.0	375.0	527.0
Orthophosphate (phase 1)	mg P L ⁻¹	1	0.2	0.2	0.3
		2	0.3	0.2	0.3
Orthophosphate (phase 2)		1	0.5	0.5	0.6
		2	0.6	0.5	0.7
pH		1	7.3	7.1	7.4

Parameter	Unit	Zone	Median	Lower quartile	Upper quartile
Temperature	C	2	7.4	7.3	7.6
		1	12.5	7.1	17.8
Total Alkalinity	mg CaCO ₃ L ⁻¹	2	10.5	6.5	17.4
		1	23.0	21.0	25.0
Total Aluminum	μg L ⁻¹	2	19.0	16.0	21.0
		1	11.0	9.2	13.0
Total Iron		2	38.0	23.0	70.8
		1	25.0	25.0	25.0
Total Lead		2	25.0	25.0	25.0
		1	59.0	36.0	95.5
Total Manganese		2	85.0	26.8	190.0
		1	1.0	1.0	2.5
Total Zinc		2	3.2	2.3	4.9
		1	180.0	150.0	220.0
Turbidity	NTU	2	190.0	160.0	210.0
		1	0.1	0.1	0.2
		2	0.1	0.1	0.2

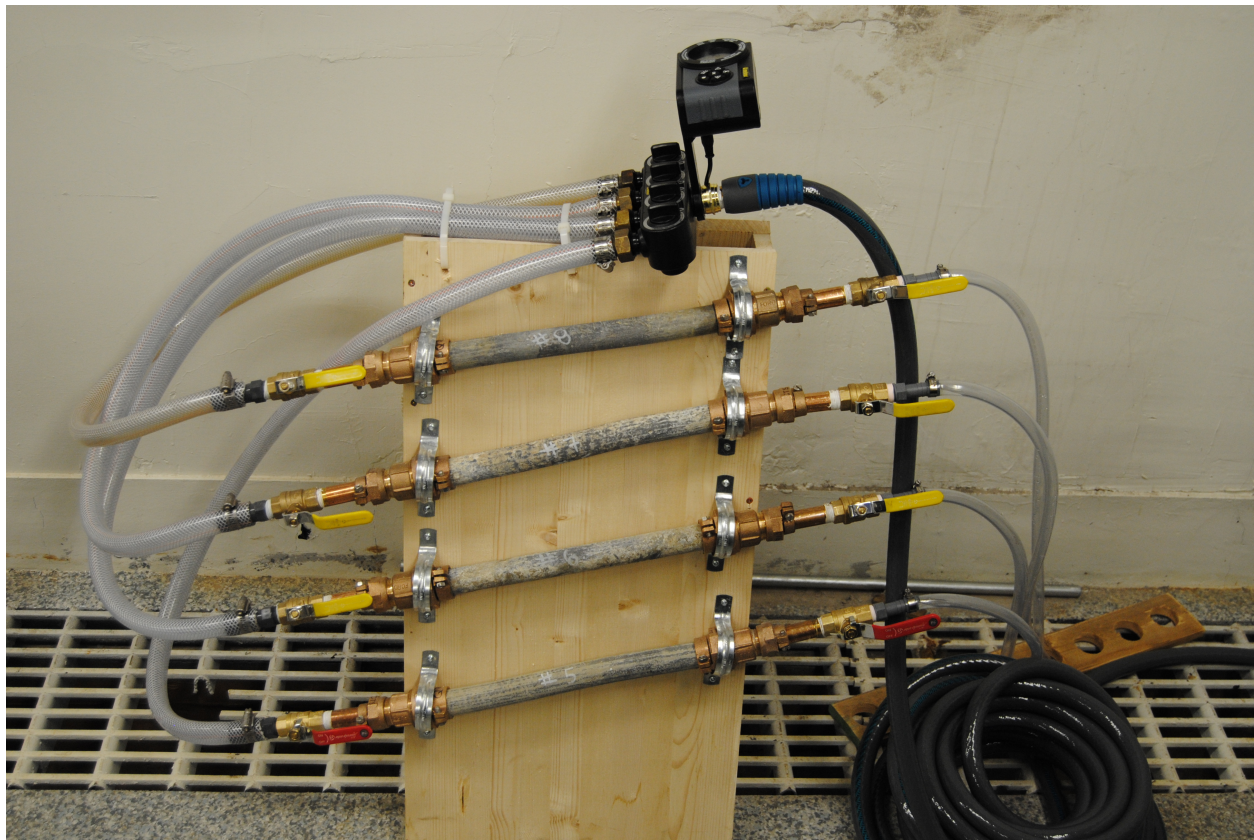
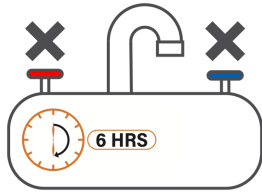


Figure S1. An example of the pipe racks installed in Zones 1 and 2.

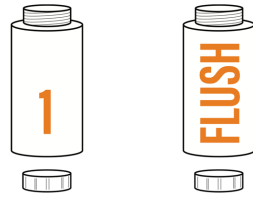
Sampling Instructions

Participation ID: 0817
Event ID: 2021

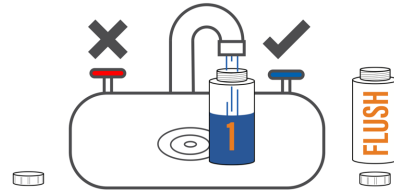
Category		Sample Kit Type	
<input type="checkbox"/> B4	<input type="checkbox"/> 9M	<input checked="" type="checkbox"/> LC-2	<input type="checkbox"/> LC-5
<input type="checkbox"/> 3M	<input type="checkbox"/> 12M	<input type="checkbox"/> NA	<input type="checkbox"/> NA
<input type="checkbox"/> 6M	<input checked="" type="checkbox"/> NA	For internal use only.	



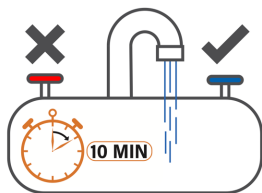
1 Ensure no water has been used in your home for 6-hours.



2 Identify Bottle 1 and place it near the faucet with the cover removed. Set the Flush bottle to the side for use in Step #6.



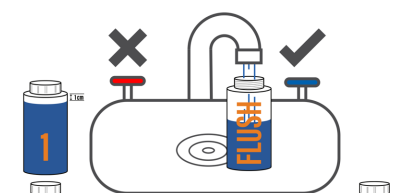
3 Place bottle #1 under the tap and turn on only the cold water tap and fill bottle #1. Do not adjust the tap, allow it to continue running. Leave about 1 cm of the bottle empty at the top.



4 Continue to run cold water through the same faucet for at least ten minutes.



5 Record the date, time, and faucet location for bottle #1 on the Lead Sample Kit Collection Information form.



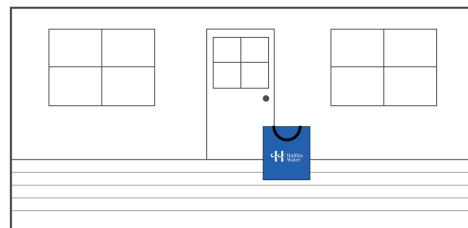
6 Without adjusting the tap, fill the Flush bottle, leaving about 1 cm of the bottle empty at the top. Turn off the faucet once the Flush bottle is full.



7 Record the date, time, and faucet location for the Flush bottle on the Lead Sample Kit Collection Information form.



8 Note your assigned sample kit pick-up date.



9 Place both full bottles inside the bag provided and leave the sample kit on your doorstep for Halifax Water to pick up on the assigned pick-up date (Step 8). * please leave samples out by 8am

902.292.2437 450 Cowie Hill Road, Halifax, NS B3P 2V3 leadandcopper@halifaxwater.ca



Figure S2. An example instruction sheet distributed to volunteer residents collecting point-of-use samples from sentinel homes.

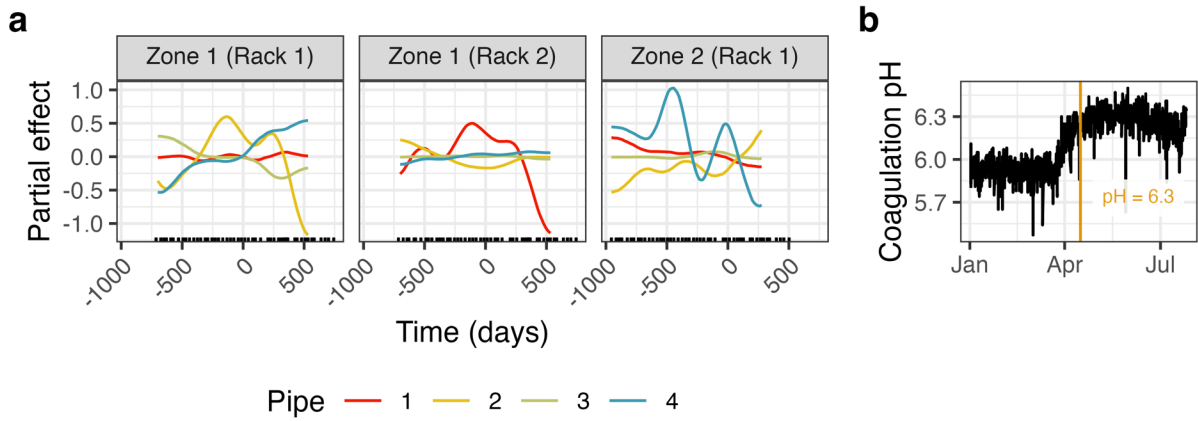


Figure S3. (a) In the full (Zones 1 and 2) model, local multi-year smooths capturing the deviations of each series from the global and location-specific smooths. **(b)** Coagulation pH at the treatment plant supplying Zone 2.

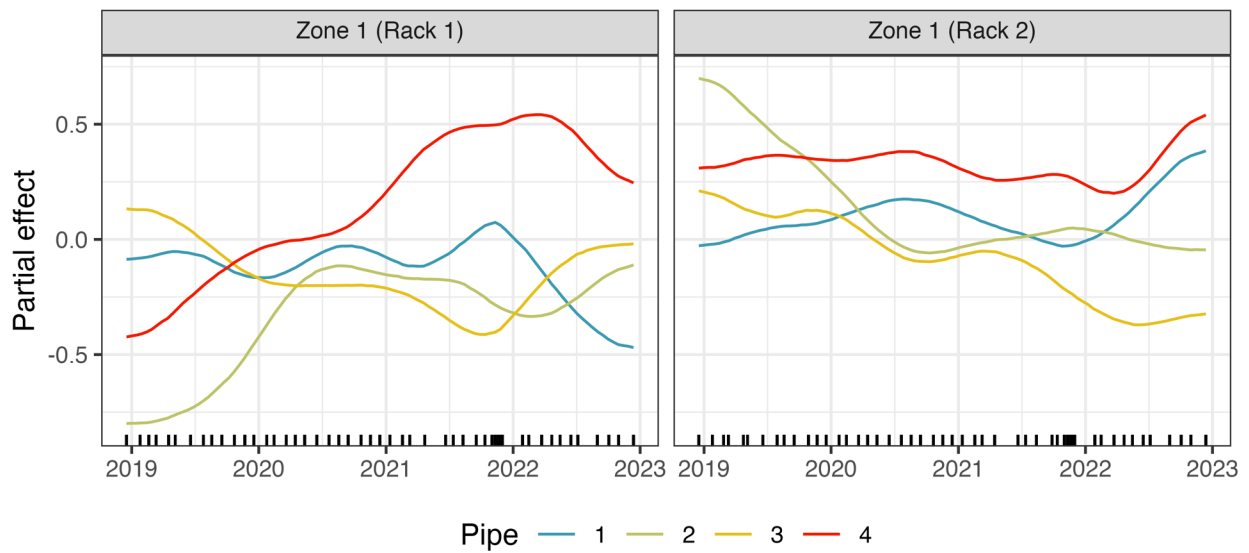


Figure S4. In the Zone 1 model, local multi-year smooths capturing the deviations of each series from the global and seasonal smooths.

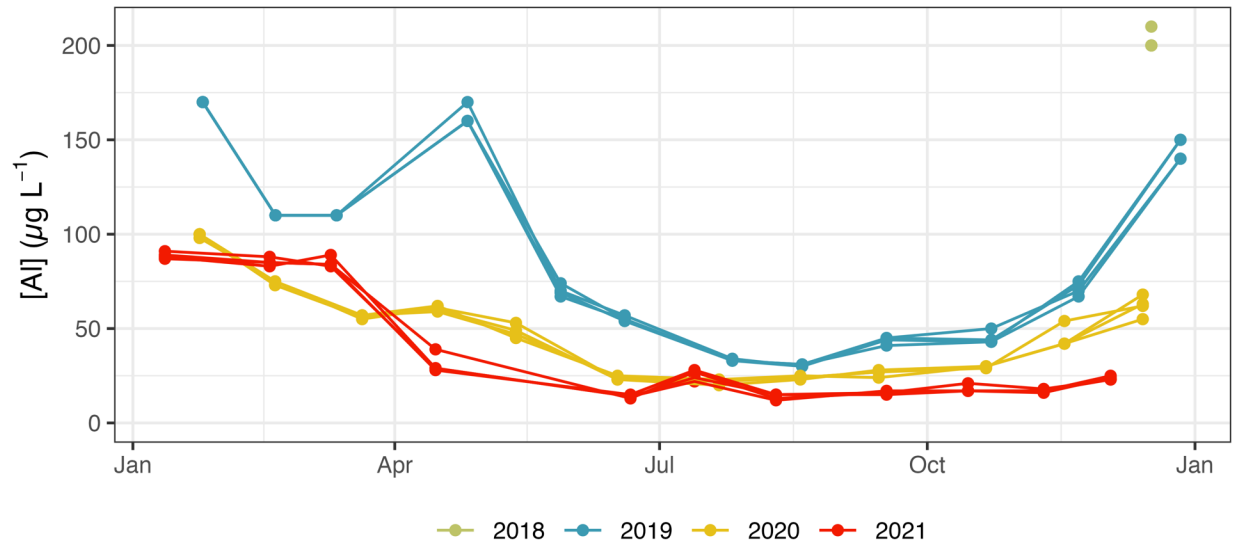


Figure S5. Total aluminum in pipe rack effluent.